Unclassified

AD-A234 965

JMENTATION PAGE

Form Approved
OMB No. 0704-0188

1b. RESTRICTIVE MARKINGS

3. DISTRIBUTION/AVAILABILITY OF REPORT
Approved for public release: distribution unlimited

2b. DECLASSIFICATION/DOWNGRADING SCHEDULE

4. PERFORMING ORGANIZATION REPORT NUMBER(S)

5. MONITORING ORGANIZATION REPORT NUMBER(S)

DTIC ELECTE APR 19 1991 S E D

6a. NAME OF PERFORMING ORGANIZATION
National Institute of Standards & Technology

6b. OFFICE SYMBOL (If applicable)

7a. NAME OF MONITORING ORGANIZATION
Office of Naval Research

6c. ADDRESS (City, State, and ZIP Code)
Ultrasonic Standards Group, Sound-A147
Gaithersburg, MD 20899

7b. ADDRESS (City, State, and ZIP Code)
Physics Division - Code 1112
Arlington, VA 22217-5000

8a. NAME OF FUNDING/SPONSORING ORGANIZATION

8b. OFFICE SYMBOL (If applicable)

9. PROCUREMENT INSTRUMENT IDENTIFICATION NUMBER
N00014-90-F-0001

8c. ADDRESS (City, State, and ZIP Code)

10. SOURCE OF FUNDING NUMBERS

PROGRAM ELEMENT NO.	PROJECT NO.	TASK NO.	WORK UNIT ACCESSION NO.
61153N		4126303	

11. TITLE (Include Security Classification) Progress in Ultrasonic Measurements Research in 1990: Transient Sources for Acoustic Emission Work (Unclassified)

12. PERSONAL AUTHOR(S)
F.R. Breckenridge, T.M. Proctor, N.N. Hsu, S.E. Fick, D.G. Eitzen

13a. TYPE OF REPORT	13b. TIME COVERED	14. DATE OF REPORT (Year, Month, Day)	15. PAGE COUNT
Annual Summary	FROM 891001 TO 900930	900821	18

16. SUPPLEMENTARY NOTATION This paper summarizes the work in Ultrasonic Measurements Research in FY-90 and will be presented in Japan at the International AE Symposium (1990).

17. COSATI CODES		
FIELD	GROUP	SUB-GROUP
20	01	
17	01	

18. SUBJECT TERMS (Continue on reverse if necessary and identify by block number)
Ultrasonics, physical acoustics, acoustic emission, transducers, non-destructive testing.

19. ABSTRACT (Continue on reverse if necessary and identify by block number)

Many techniques have been used by acoustic emission workers to produce rapid transient disturbances in elastic media. Techniques employing transient sources are necessary for characterizing many acoustic emission system components such as receiving transducers, transfer media, and other sources as well.

Wave forms from seven types of sources were studied by performing experiments in which the source and a high fidelity receiver were mounted on opposite sides of an aluminum plate. Soundspeeds in the plate had been previously measured to provide information necessary for the calculation of the plate Green's function. In each experiment, a source was triggered and the ensuing output from the receiver was captured by a transient recorder. The force waveform of the source was calculated by convolving the inverse of the plate Green's function with the captured waveform.

20. DISTRIBUTION/AVAILABILITY OF ABSTRACT
☒ UNCLASSIFIED/UNLIMITED ☐ SAME AS RPT ☐ DTIC USERS

21. ABSTRACT SECURITY CLASSIFICATION
UNCLASSIFIED

22a. NAME OF RESPONSIBLE INDIVIDUAL
L.E. Hargrove, ONR Physics Division

22b. TELEPHONE (Include Area Code) 202-696-4221

22c. OFFICE SYMBOL
ONR Code 1112

DD Form 1473, JUN 86

Previous editions are obsolete

SECURITY CLASSIFICATION OF THIS PAGE
UNCLASSIFIED

91 4 18 016

Accession For
NTIS GRA&I
DTIC TAB
Unannounced
Justification
By
Distribution/
Availability Codes
Dist | Avail and/or Special
A-1

PROGRESS IN ULTRASONIC MEASUREMENTS RESEARCH IN 1990: TRANSIENT SOURCES FOR ACOUSTIC EMISSION WORK

F.R. BRECKENRIDGE, T.M. PROCTOR, N.N. HSU, S.E. FICK, D.G. EITZEN

National Institute of Standards and Technology
Gaithersburg, Maryland 20899, U S A

ABSTRACT

Many techniques have been used by acoustic emission workers to produce rapid transient disturbances in elastic media. Techniques employing transient sources are necessary for characterizing many acoustic emission system components such as receiving transducers, transfer media, and other sources as well.

Waveforms from seven types of sources were studied by performing experiments in which the source and a high fidelity receiver were mounted on opposite sides of an aluminum plate. Soundspeeds in the plate had been previously measured to provide information necessary for the calculation of the plate Green's function. In each experiment, a source was triggered and the ensuing output from the receiver was captured by a transient recorder. The force waveform of the source was calculated by convolving the inverse of the plate Green's function with the captured waveform.

This paper is a compilation of information about the following types of sources: pencil, capillary, capacitive transducer, conical transducer, ball impact, spark, and high explosive. Force waveforms and other relevant data concerning the sources are given and comments made on their relative merits. The ideal source would be infinitesimal in size, have a simple force waveform such as a step or delta function, and would have a relatively large amplitude which could be determined from a priori considerations. None of the sources considered in this paper approach perfection in all of these respects. Hence, the choice of a source for a particular purpose will involve tradeoffs based on the particular merits of each source.

INTRODUCTION

Many different kinds of transient sources[1-8] have been used, in acoustic emission experiments, to create orderly wavetrains (simulated acoustic emission) used for characterizing acoustic emission equipment, transducers or propagation media. Unlike true acoustic emission, which usually originates in the interior of a solid medium, the waves generated by the sources considered here are launched from the surface. The work reported in this paper constitutes an attempt to develop detailed quantitative information about the performance of seven different means of creating simulated acoustic emission.

In the interests of simplicity, the sources are described by the forces they induce at the wave-launching surface. In general, the characteristics of such forces will be determined by the properties of both the sources themselves and the propagation media. For this study, we used one medium, 2017-T4 aluminum, with all the sources to allow direct comparisons of the data but made no attempt to predict the performance of the sources on other media, or in general.

THEORY OF THE EXPERIMENT

The complex behavior of elastic waves in solid media dictates that even the simplest schemes for determining transient-source characteristics be somewhat complicated[9,10]. For this experiment we used the results of recent theoretical work[11,12] to calculate the force-time data for the sources from voltage-time data from a high-fidelity receiving transducer. Such calculations are possible only for a few specific propagation-medium geometries, of which we used the infinite plate for our work. The expression for the source force-time waveform S is:

$$S = E*G^{-1}*R^{-1}*A^{-1}, \qquad (1)$$

where E is the voltage waveform from the receiving transducer,
G is the transfer function of the plate (Green's function G_{33}),
R is the impulse response function of the receiving transducer,
A is the impulse response function of the receiver electronics,
and * denotes convolution. The functions R and A are computed from the results of electrical measurements, and the inverses found by direct time domain deconvolution[11,12]. Although this inversion method does not necessarily give stable results in the general case[13], the data underlying R,A, and G can be modified without significant loss of information to ensure stable inversion.

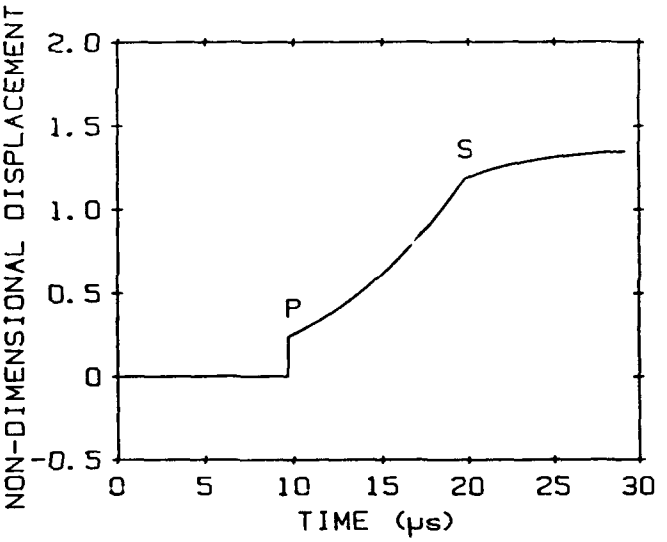

Figure 1A. Transfer function for the aluminum plate based on elasticity theory, from measured values: longitudinal speed = 6.3633 km/s, shear speed = 3.1374 km/s, length = 0.06209 m, and assuming $\mu = 2.558 \times 10^{10}$ N/m.

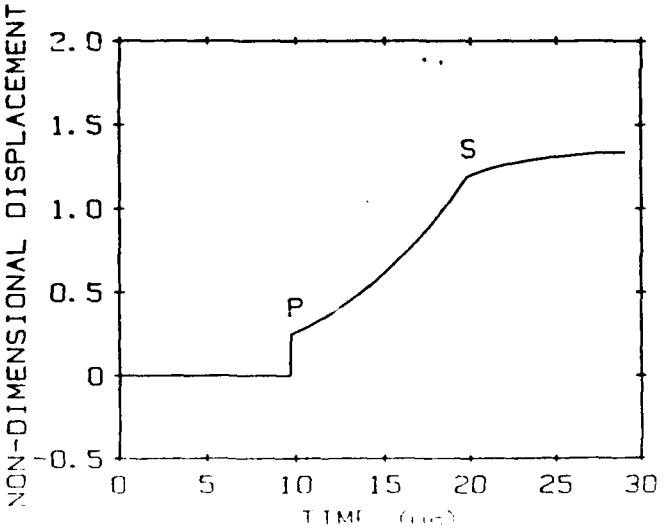

Figure 1B. Transfer function for the aluminum plate determined from an experiment using a capacitive source and a capacitive receiver.

The plate transfer function, G, can be calculated using elasticity theory[14,15], and can also be derived from the results of experiments[16] involving a source with independently known transfer function. During preliminary work, G was determined both theoretically, and from experimental data obtained using a well-characterized capacitive source transducer. Each of the two different versions of G was then used to compute S, the force-time waveform, for the pencil source and the capacitive source. Note that the two transfer functions shown in Figure 1 are nearly identical. Unlike the G functions themselves, the force-time waveforms were significantly different--the results obtained using the theoretically derived G function showed anomalies which were not as large in the results based on the experimentally derived G function. We take this to mean that the experimentally-derived G function reflects the effects of local inhomogeneities and other real-world artifacts which are not taken into account by the elasticity theory underlying the theoretical G function. Accordingly, we used the experimentally derived G function in computing the results reported throughout this paper.

PRACTICAL DETAILS

The infinite plate was realized in our experiments by an aluminum cylinder 177 mm in diameter and 62 mm long, with polished ends. The cylinder was used with its axis vertical, and with source and receiver located at the centers of the top and bottom end faces, respectively (Figure 2). The size of the plate was chosen to provide a working time of 19.5 μs, limited by reflections from the cylindrical surface. Since all data were terminated prior to the arrival of these reflections at the receiver, infinite plate theory is applicable.

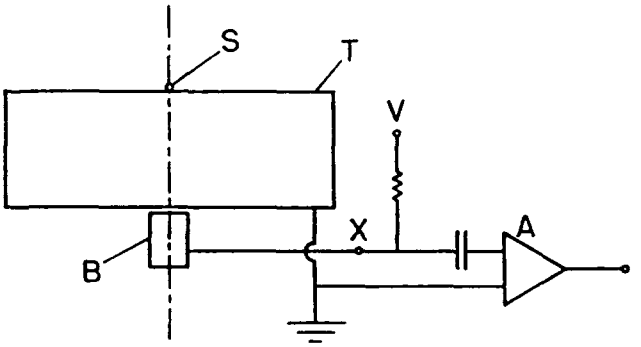

Figure 2. Experimental setup: S, source; T, aluminum transfer plate; B, capacitive receiver; A, charge amplifier. Polarizing voltage applied at V. For amplifier calibration, charge injected at X with receiver disconnected.

A charge amplifier, and in some cases an additional gain stage, amplified the received signal for digitization by a waveform recorder. Data processing was done using a "PC"-type computer. Descriptions of further experimental detail accompany the particulars for each type of source.

STANDARD CAPACITIVE SOURCE AND RECEIVER

Capacitive receivers have been used by workers in the acoustic emission field[2,17-20], but capacitive devices have seldom been found practical as sources[3]. We constructed a special air-gap capacitive transducer which functions as a high fidelity displacement sensor and a similar device which functions as a high fidelity source. These two transducers were used to establish the transfer function of the plate.

A major constraint in the use of a capacitive transducer having an air gap of only a few micrometers is that the gap must be parallel, controlled in thickness[19], and not contain any dirt which might alter the gap or short out the transducer. The present design embodies features which allow these requirements to be met relatively easily. The capacitive source consists of a cylindrical brass backplate, approximately 5 mm in diameter by 10 mm long, held in position near the transfer plate, with one flat end polished and parallel to the face of the transfer plate. The device supporting the backplate is designed to electrically isolate the backplate from the transfer plate, and to allow fine adjustment of the width and parallelism of the air gap between the backplate and the transfer plate. The supporting device also acts as a compliant member between the transfer plate and the backplate so that, for the frequency range of interest, the backplate is held fixed in space by its own inertia. The measured primary resonance of the transducer was at 1.52 kHz, which is low enough to have a negligible effect on the source waveform.

The desired width and parallelism of the air gap are established by temporarily placing the transducer assembly on a glass optical flat illuminated by monochromatic light and equipped with a mirror underneath to allow viewing of the air gap by looking through the optical flat. The gap is decreased by pushing down on the transducer until the fringe pattern indicates contact; then, while slowly releasing the downward force, the increase in gap width can be determined by counting the fringes. Fine adjustments are made using the three screw and lever mechanisms which individually adjust the three feet (Figures 3 and 4).

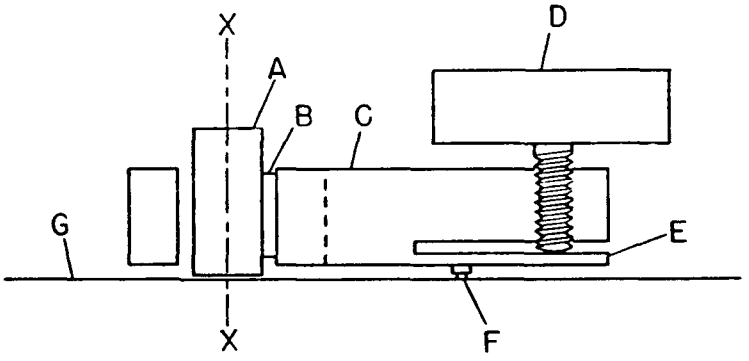

Figure 3. Standard capacitive source transducer, longitudinal section: A, cylindrical brass backplate, axis X-X; G, transfer block. Located with threefold symmetry about X-X are: B, glass insulator; C, support arm; D, anti-backlash adjusting screw; E, bending leaf spring; F, foot.

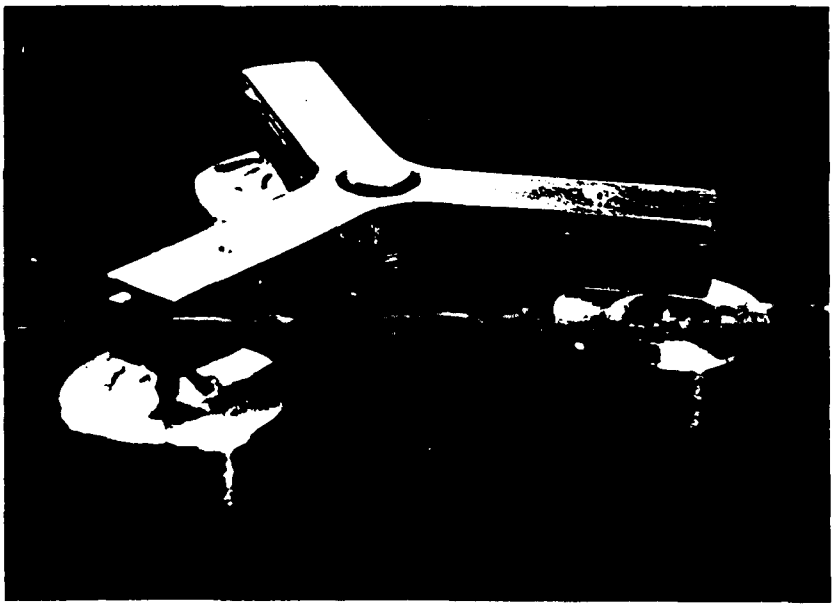

Figure 4. Standard capacitive source transducer, upside down.

The step force used in experimentally determining the plate transfer function was generated by connecting a charged capacitor to the transducer using the circuit shown in Figure 5. Calculation of the force generated by the source transducer is set forth in Appendix A.

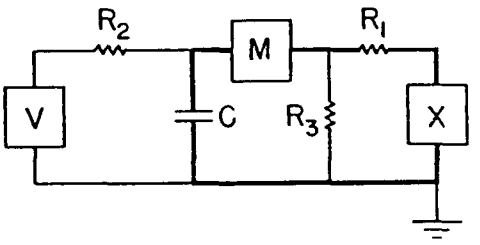

Figure 5. Driver circuit for capacitive and conical sources: V, voltage supply; X, transducer (Ground electrode is the plate.); M, mercury wetted reed relay; C, storage capacitor; damping resistor R_1 = 27.4 ohms; isolation resistor R_2 = 1.5 k; bleeder resistor R_3 = 357 ohms. Heavy lines denote low inductance construction.

The capacitive receiver transducer differs from the source transducer mainly in the size of the backplate and the design of the three levelling supports. The technique of adjusting and measuring the gap is the same. In the receiver, the backplate is made of tungsten and is about 10 mm in diameter by 25 mm long. The primary resonance of this transducer, at 1.48 kHz, is low enough not to affect the results of our experiments significantly.

Since the transducer was used on the bottom of the plate, special mounting arrangements were required. A lever was constructed with an adjustable counterweight, low friction pivot bearings, and a gimbal assembly to allow freedom of motion of the transducer for proper seating. Before the transducer-and-lever assembly was positioned under the plate, the counterweight was adjusted so that the net force holding the transducer against its mounting surface would be the same as it was when the gap was adjusted using the optical flat.

In designing the receiver, the choice of backplate diameter is subject to the following considerations: The sensitivity is proportional to the area, but the risetime, limited by the arrival of oblique rays at the edge of the backplate, increases with the square root of the diameter. The 1 cm diameter chosen for this work resulted in a risetime of 30 ns. The spectral distribution of the front-end noise is dependent on capacitive loading; with the transducer connected, the noise floor was equivalent to about 10^{-13} m rms at 8 MHz bandwidth.

The circuit (Figure 2) associated with the capacitive receiver is a conventional one using a charge amplifier. The charge sensitivity of the capacitive receiver is readily calculated, as shown in Appendix B. To determine the impulse response function (A in Equation (1)) of the receiver electronics under the conditions of actual use, a transient capture was made with the transducer replaced at the terminal X of Figure 2, by a circuit of identical impedance designed to inject a known charge impulse.

TREATMENT OF THE SOURCE WAVEFORM DATA

For each of the source waveforms studied, one or more transient data records consisting of 512 samples of ten bit data were made. For sources that could be repeated readily, multiple records were averaged. Figure 6 shows a typical captured waveform record from a pencil source. Numerical convolution of the captured record with the system inverse response function yielded the true force waveform of the source. Figure 7B shows the pencil-source waveform derived from the waveform of Figure 6; the lack of flatness of the waveform

following the rise may have resulted from imperfection of the experimental transfer function, or might indicate that the pencil force had a sideways component.

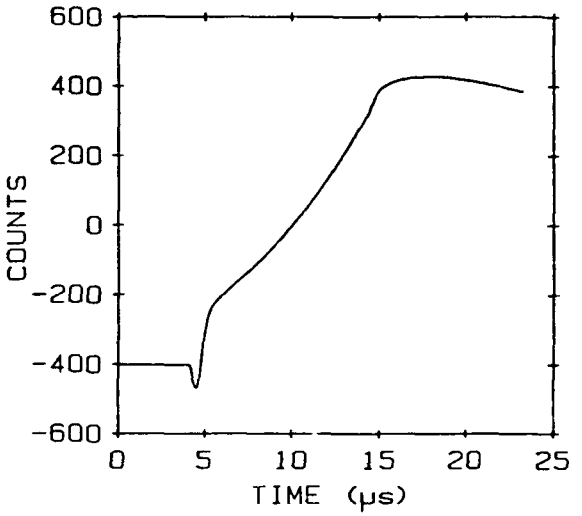

Figure 6. Captured waveform from a 0.3 mm pencil source.

The spectra shown in this paper are modified discrete Fourier transforms of derived time-domain force waveforms. The time domain data were adjusted by subtracting a linear ramp parameterized to bring about equality of initial and final data points[21], in order to eliminate spurious spectral components.

High frequency rolloff in the unmodified spectra was countered by multiplying the value for each frequency by the angular frequency,ω; this process keeps the graphs on scale at all frequencies. The effect of multiplication by ω is the same as that of differentiating the time-domain data. A flat spectrum therefore corresponds to a step function of force, and 0 dB on the spectral graphs corresponds to a 1 newton step.

ACCURACY

The accuracy of the magnitudes of all of the force waveforms depends mainly on the accuracy of the determination of the 0.709 N step force generated by the standard capacitive transducer in the experimental determination of the plate transfer function G. This step force is given by $S_{Std} = C^2V^2/2\epsilon A$ (Appendix A). The error limits are given in Table I. Additional errors introduced by the digitizing process of the waveform recorder and by the calculations may introduce noise in the data, and cause the spectral results to be erratic, but should not significantly bias the magnitudes of the time waveform data. Accordingly, the error bounds for the force waveforms are the same as the error bounds for S_{Std}.

Table I. Error Limits for S_{Std}

Quantity (Error Type)	Estimated Error (%)	Error Contribution to S_{Std} (%)
C (measurement)	±2.5	±5
C (fringing C)	0 to +2.5	0 to +5
V	±0.2	±0.4
A	±1	±1
Total (worst case)	-	-6.4 to 11.4

For two of the sources, force waveforms can be computed without recourse to receiver data. The estimated accuracies of these independent methods, and of the method involving the theoretically-determined plate transfer function G, are shown in Table II. The discrepancies are the average percentages by which the force waveforms reported in the paper exceeded the average force values computed using the other methods. Taking all evidence into consideration, the reported force waveforms are thought likely, at worst, to be high by a few percent.

Table II. Alternative Force Determinations

Alternative Method	Discrepancy (%)	Estimated Accuracy Alternative Force Determination (%)
Glass Capillary	+4.0	±5
Ball Impact	+1.5	±5
Transfer Function Theory	-5.0	-8 to +13

PENCIL SOURCE

The breaking of a pencil lead against the surface of the transfer plate produces a sudden step-like release of compressive force with a total (0 to 100%) risetime of about 2.5 μs. The magnitude of the step depends on the size, hardness and extension of the lead beyond the pencil collet. An interesting feature of the waveform is that it begins with compression, rather than with compression release. This can be explained by considering that, after the lead fractures near the collet, various waves propagate along the lead at different speeds. The wave arriving at the plate first is longitudinal, and results in a momentary increase of compressive force prior to the ultimate release of all compressive force. Pencils having lead diameters of 0.2 mm, 0.3 mm, and 0.5 mm were tested, and force values between 1 N and 5 N were measured (Figure 7).

Each of the spectra corresponding to the three force waveforms contains a null at a frequency approximately proportional to the inverse of the lead diameter. At higher frequencies the results appear erratic.

GLASS CAPILLARY SOURCE

In our experiments, glass capillary tubing was squeezed between the surface of the transfer plate and a glass rod, 4 mm in diameter, oriented with its axis parallel to the surface of the plate and perpendicular to the axis of the capillary. The force was produced by a screw which pushed against the glass rod. The screw contained a peizoceramic force sensor which had been calibrated using known weights.

Three samples of capillary tubing were investigated. Two of them were pulled from laboratory Pyrex tubing having an original size of about 5 mm; the third was commercial capillary tubing made of Owens-Illinois KG-33 heat resistant glass[22]. A typical waveform from the Pyrex tubing and the corresponding spectrum are shown in Figure 8. The average discrepancy between the force as estimated from the force waveforms and the force reading of the loading screw transducer was 4%, the waveform giving the higher value.

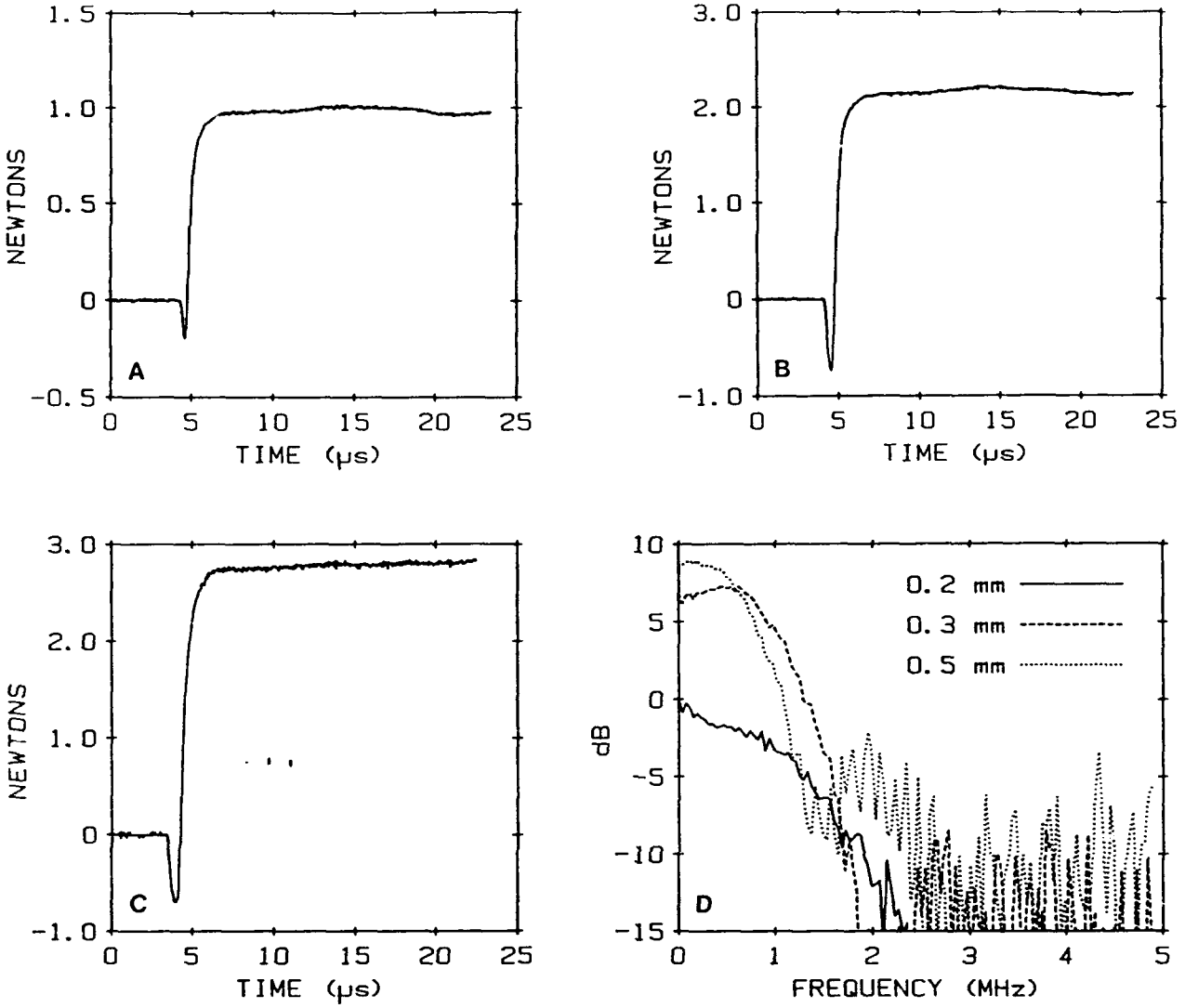

Figure 7. Pencil source: A. Waveform from 0.2 mm lead. B. Waveform from 0.3 mm lead; C. Waveform from 0.5 mm lead (JSNDI-006 pencil and lead). D. Spectra corresponding to A,B,C.

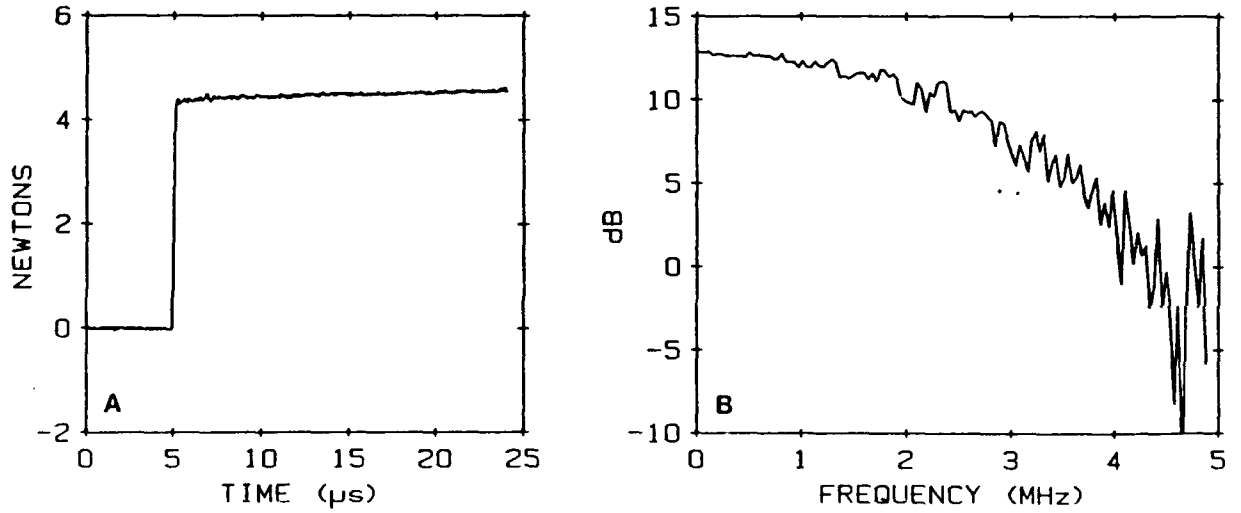

Figure 8. Glass capillary source: A. Waveform from 0.117 mm capillary. B. Corresponding spectrum.

In general, the magnitude of the force depended mainly on the ratio of the bore to the outside diameter of the tubing, but also on the material and the diameter. In our experience, the ratio that produces the most consistent results is one half. Using tubing of this ratio and various diameters, a wide range of breaking strengths can be achieved--the larger the tubing, the greater the strength, but the slower the rise. Of the two materials tested, the Pyrex produces somewhat larger forces. Capillary sources are capable of step forces of 25 N or more. Here, we used step forces no greater than about 5 N to avoid overloading of the charge amplifier.

CAPACITIVE TRANSDUCER SOURCE

The construction of the standard capacitive source transducer has been described above. For this device, 64 transient captures were averaged to produce the force waveform and the spectrum of Figures 9A and 9B, respectively. The nearly perfect step-like shape of the waveform, and the agreement of its magnitude with the 0.0709 N value calculated independently for the transducer, are consistent with the assumptions used in calculation of the plate transfer function.

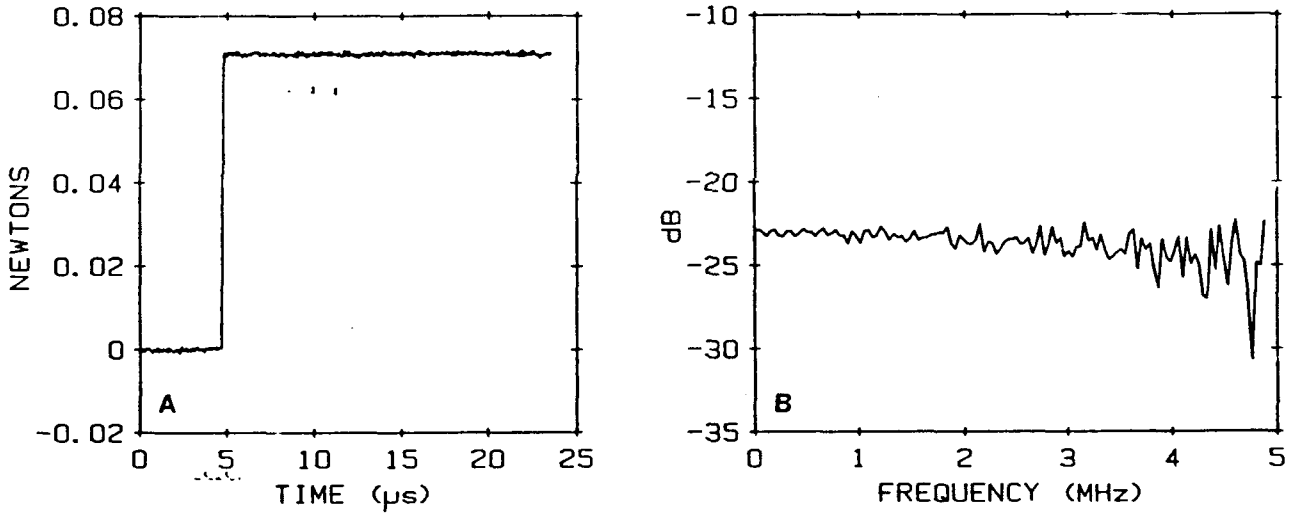

Figure 9. Standard Capacitive Transducer source: A. Waveform from the standard capacitive source transducer, in the circuit of Figure 5, driven with a 49.7 V step. B. Corresponding spectrum.

A simpler type of capacitive transducer uses a layer of plastic film in the interelectrode gap. The disadvantages of this transducer are that its resonance frequency is higher than that of a similar air-gap capacitor, and various frequency dependent effects are introduced by the dielectric film. If polarizing voltage is applied to the transducer, its sensitivity is high at first, but decreases with time after the onset of the applied voltage because of reverse polarization effects in the dielectric, causing the sensitivity of the transducer to be unstable. In its favor, the device can withstand higher voltages than an air-gap capacitor of the same dimensions, and is capable of producing force waveforms with equally fast rise. Figure 10 shows a force waveform (from 32 captures) produced by a transducer of this type when driven by a 200 V step (circuit of Figure 5). The progressive sag of the waveform is actually the beginning of a sinusoidal oscillation at the natural resonance frequency of the transducer.

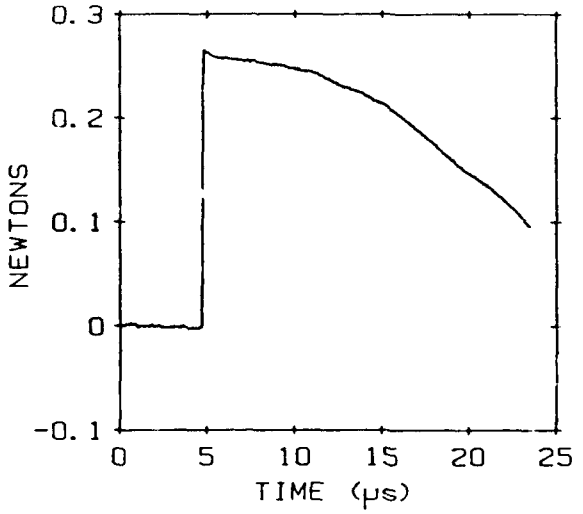

Figure 10. Waveform from a capacitive source employing 4 μm thick polycarbonate dielectric and 5 mm diameter by 10 mm long cylindrical brass backplate, driven with a 200 V step. Corresponding spectrum resembles 9B, but with higher magnitude.

CONICAL TRANSDUCER SOURCE

The conical transducer designed at NBS for use as a high-fidelity receiver[23,24] may also be used as a source[4]. Two such transducers, designated #4 and #5, were tested as sources driven by voltage steps produced using the circuit of Figure 5. Driven by a 100 volt step, transducer #5 generated the waveform, an average of 32 captures, shown in Figure 11A; the corresponding spectrum is shown in Figure 11B. The fine structure evident in both time and frequency-domain representations of the data is attributable to the various mechanical resonances of the conical transducer element and backing block. The conical transducer delivers about 0.01 newton per volt and is capable of withstanding as much as 1 kV.

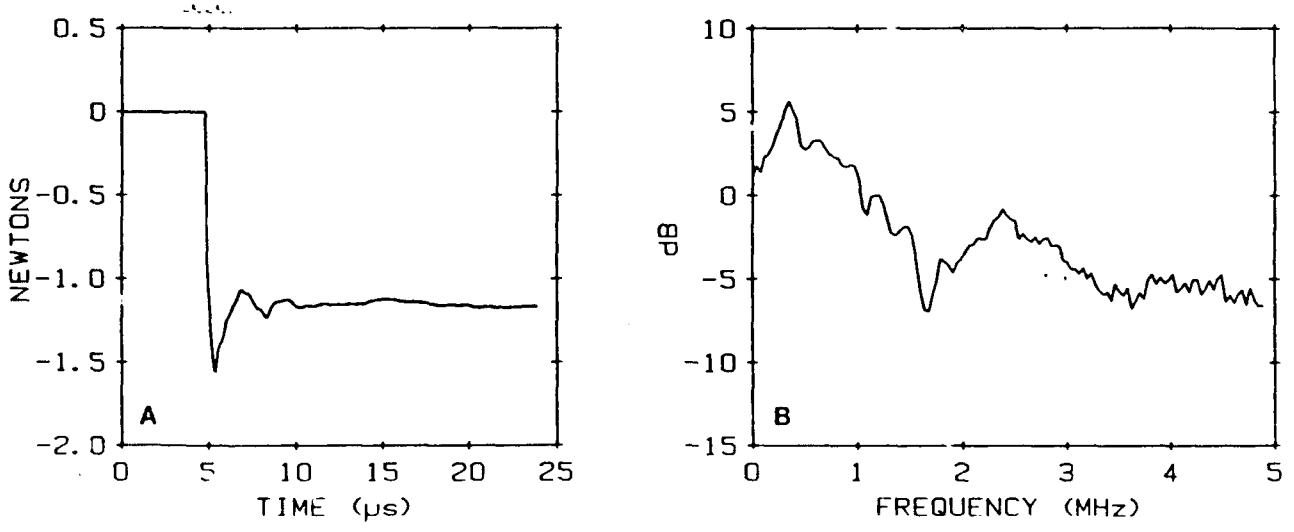

Figure 11. Conical transducer #5, driven with a 100 V step: A. Waveform. B. Corresponding spectrum.

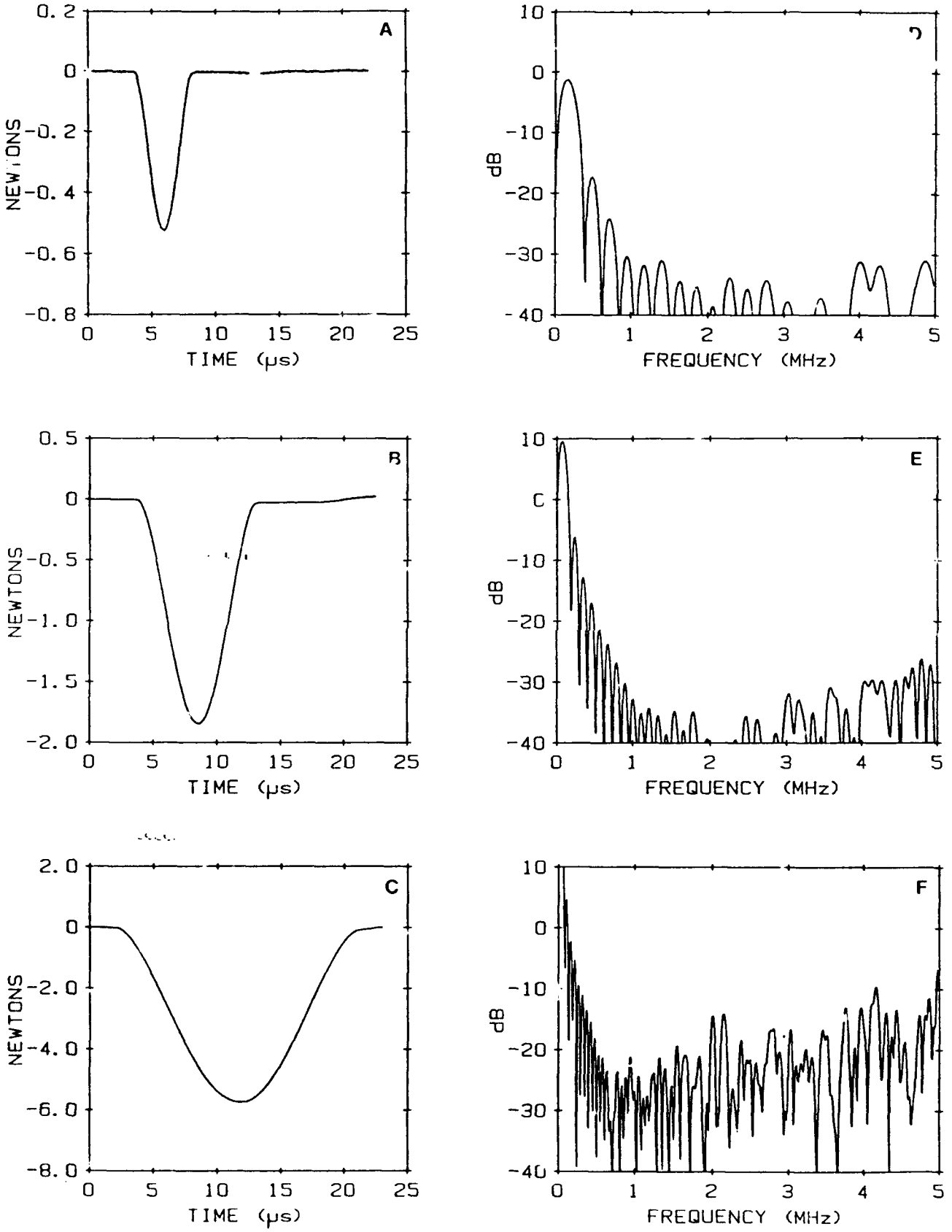

Figure 12. Ball impact source: A. Waveform from 0.794 mm ball. B. Waveform from 1.587 mm ball. C. Waveform from 3.175 mm ball. D-F Spectra corresponding to A-C.

BALL IMPACT SOURCE

The collision of a sphere and a plate produces an impulsive force quite different from the step-like forces produced by the sources described earlier in this paper. The theory of elastic sphere impact has been treated by Hertz[25] and Goldsmith[26]. Non-elastic impact forces have been measured experimentally[27] and flaw detection in concrete[6] has been done using a ball-impact source. Thorough experimental investigations of elastic ball-impact forces have already been made[5,28]; the experiments reported here were undertaken mainly to broaden the base of empirical data applicable to our particular setup.

Hardened steel balls, manufactured for use in ball bearings, were dropped from a vacuum holder from heights of a few millimeters. Numerical results extracted from the waveform data of Figure 12A-12C are shown in Table III. The reported values of measured impulse were obtained by numerical integration of force waveform data, while values of calculated impulse were based on photographic measurements of rebound heights. On average, the measured values were higher than the calculated values by 1.5%. Inelasticity was evidenced by dents in the plate and by the rebound height measurements.

Table III: Summary of Ball-Source Results

Ball Diameter (mm)	0.79	1.59	2.38	3.18
Number of Events	4	10	5	10
Drop Height (mm)	5.12	4.25	3.43	2.63
Rebound (height ratio)	0.766	0.849	0.871	0.944
Mass of Ball (mg)	2.0425	16.3	55.05	130.3
Calc Impulse (Nμs)	-1.214	-9.047	-27.60	-58.27
Meas Impulse (Nμs)	-1.272	-9.149	-26.97	-59.74
Meas Peak Force (N)	-0.526	-1.84	-3.53	-5.73
Meas Impulse Width (μs)	4.74	9.26	14.0	19.0

The spectra (Figures 12D-12F) have regularly spaced zeros of magnitude and reversals of phase. In each spectrum, there appears to be an envelope that bounds the peaks. If the spectra were normalized so that the drop heights for all the balls were the same, then the envelopes for all the spectra would be approximately the same. It is clear that, if continuous distribution of energy over frequency is required, say, for calibration of transducers, that the ball impact source would be a poor choice.

SPARK SOURCE

This source was realized using spark discharge between the plate and the tip of a sewing needle, connected as shown in Figure 13. In the first series of tests performed, the capacitance, C, was fixed at 1.77 nF, the damping resistor, R, was zero, and the gap was varied from 0.1 mm to 0.6 mm in increments of 0.1 mm. For each test, the voltage was slowly increased until breakdown occurred. Breakdown voltages ranged from about 1200 V to about 2100 V. In the other series of tests the voltage was fixed at 1200 V, R was 0.33 ohms, and C was varied from 1.8 nF to 9.1 nF in five steps. In each test the gap was decreased slowly to achieve breakdown. As expected, the gap at breakdown was always about the same, 0.1 mm. Monitored current waveforms had peaks ranging from 300 A to 600 A, and a total oscillatory duration of from 100 ns to 200 ns. In earlier experiments in which various values of R were used, it was found that variations in damping produced the expected effect on the spark discharge current waveform, but affected only the amplitude of the force waveform.

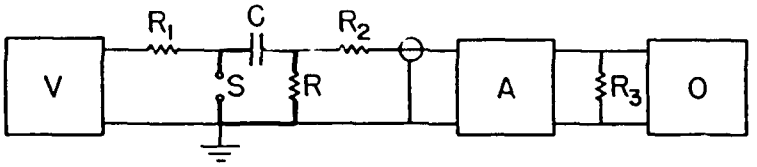

Figure 13. Driver circuit for spark source: V, high voltage supply; S, spark gap (Ground electrode is the plate.); A, 50 ohm step attenuator; O, oscilloscope. Various values used for storage capacitor C and for damping and current sensing resistor R. Isolating resistor R_1 = 22 M; terminating resistors R_2,R_3 = 50 ohms. Heavy lines denote low inductance construction.

All of the force waveforms and spectra for all tests were very similar, but varied in magnitude. A typical waveform appears in Figure 14A, while the spectra shown in Figures 14B and 14C correspond to the experiments with various gap spacings and various capacitance values, respectively.

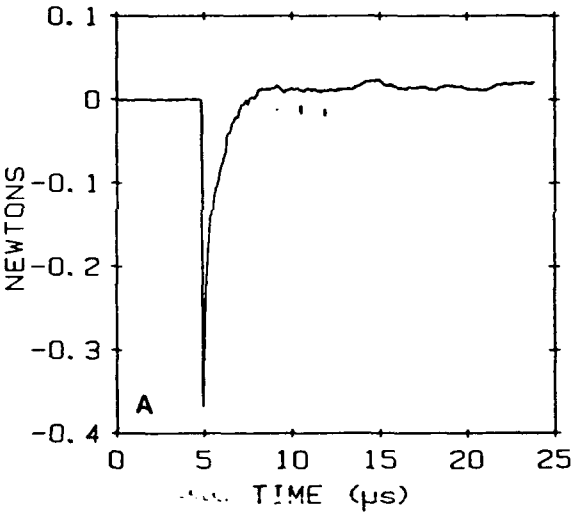

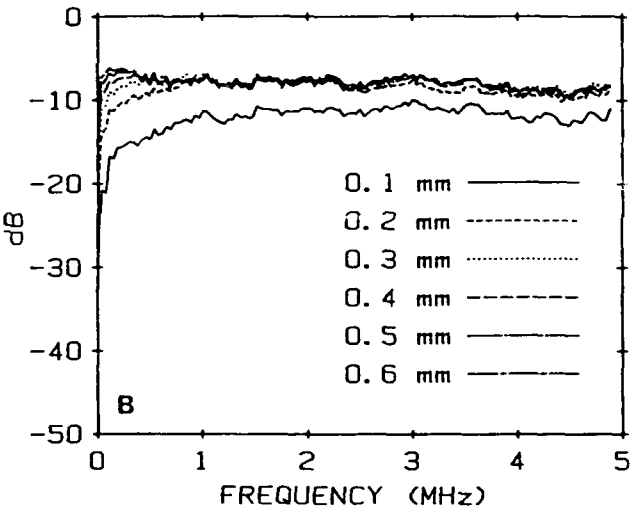

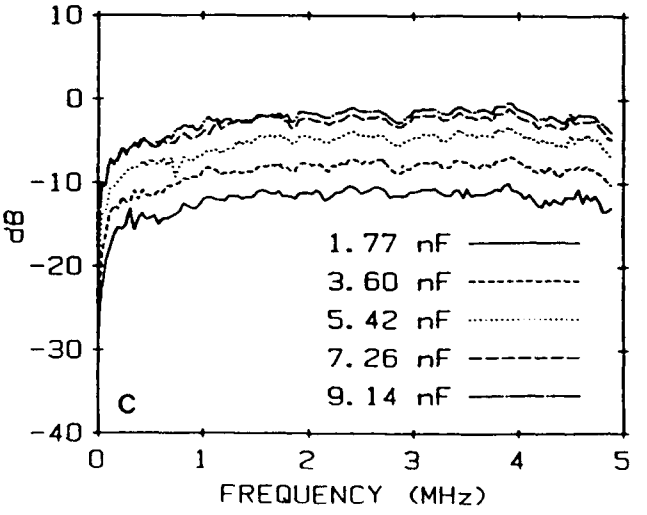

Figure 14. Spark source:
A. Typical waveform.
B. Spectra from sparks having various gap lengths.
C. Spectra from sparks discharging various values of C.

The tests for gaps of 0.3 mm and greater yielded remarkably flat spectra above 40 kHz. The main irregularity in the spectra appears to be systematically common to all, and is most likely due to some fine structure in or on the surface of the plate. Note that the set of spectra for the second series of tests also has systematic, but different, irregularities.

HIGH EXPLOSIVE SOURCE

The detonation of a very small charge of high explosive produces a fast, highly localized, high powered source. This is not a new idea; seismologists have been doing this for many years. Our experiments made use of nitrogen iodide, $NI_3 \cdot 2NH_3$, a solid which may be handled while wet, but when dry, explodes with the slightest touch[29]. A small chunk of this material, typically about 0.1 to 0.2 mm in diameter was placed on the plate while still slightly damp and allowed to dry prior to detonation.

Detonation by touching the charge with a solid object usually resulted in some undesirable transient forces being transmitted to the plate by the detonator. In later trials, we used heat from a soldering iron or a focussed 1 mW HeNe laser beam as the trigger. The resulting force waveforms showed considerable variability, which is not surprising considering the crudeness of control possible in these simple procedures. Superior performance was seen for the soldering iron triggering, perhaps because heating of the explosive charge was more uniform. Figure 15A shows one of the better waveforms obtained this way, and Figure 15B shows the spectra for all of the events triggered using the soldering iron.

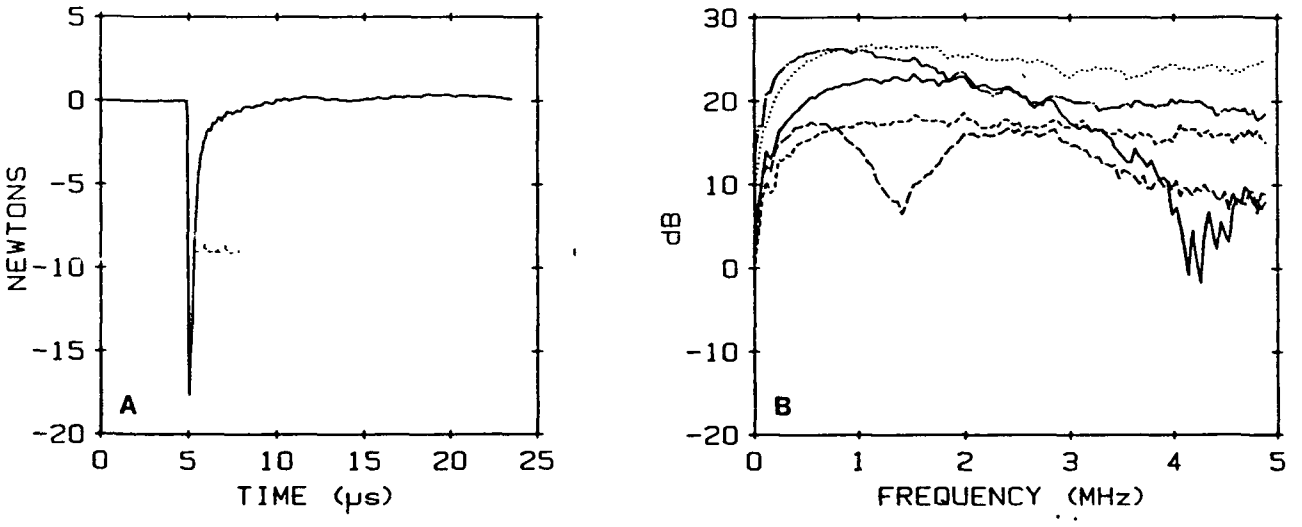

Figure 15. High explosive source: A. Force waveform from a small charge detonated by heat from nearby soldering iron. B. Spectra from five charges. The dotted curve corresponds to waveform in A.

This source provided very fast risetimes, large peak forces (sometimes exceeding 17 N) and wide, relatively flat spectra. A disadvantage that we found in using this material was that it caused pitting of the surface of the aluminum plate, possibly due to corrosion. The fact that force signature waveforms were obtained from an explosive charge may be of interest not only in NDE, but in the study of explosions.

SUMMARY

We have presented data for a wide variety of wave-generating mechanisms studied using our newest apparatus designed to exploit the scheme we believe to be the most direct method for measuring the output forces of elastic wave generators on solid media. Because the data for all seven sources were obtained under the same experimental conditions, we believe that the compiled data are good as could be obtained for the purpose of comparing the performance characteristics of the sources.

Representative data are given in Table IV. Sources which produce step-like waveforms precede those which produce impulsive waveforms. Two definitions were used in determining risetime. The 0-90% criterion is appropriate for waveforms featuring considerable high-frequency energy despite the presence of an asymptotic peak, while the full (0-100%) risetime better describes the dominant characteristic of impulsive waveforms, like those of the ball source. For each line in Table IV, the reported peak force is the average of the peak forces for the source tests described. Because the capacitively-generated forces were small enough to require the use of signal averaging, composite waveforms were synthesized from the results of 32 or 64 identical tests, and the peak force values extracted from the composite waveforms. The variations among individual waveforms for each capacitive source were small enough to be entirely attributable to electronics-related uncertainties, estimated to be less than 1% in our setup. For the other sources, the reported variation of force was determined from the ratio of the largest to the smallest peak forces obtained from a particular source under fixed testing conditions. In the reporting of all forces throughout this paper, the sign convention is that upward, or tractile, forces are positive, while downward, or compressive, forces are negative. Of all the sources tested, only the capacitive and conical transducers are capable of generating both pulse polarities.

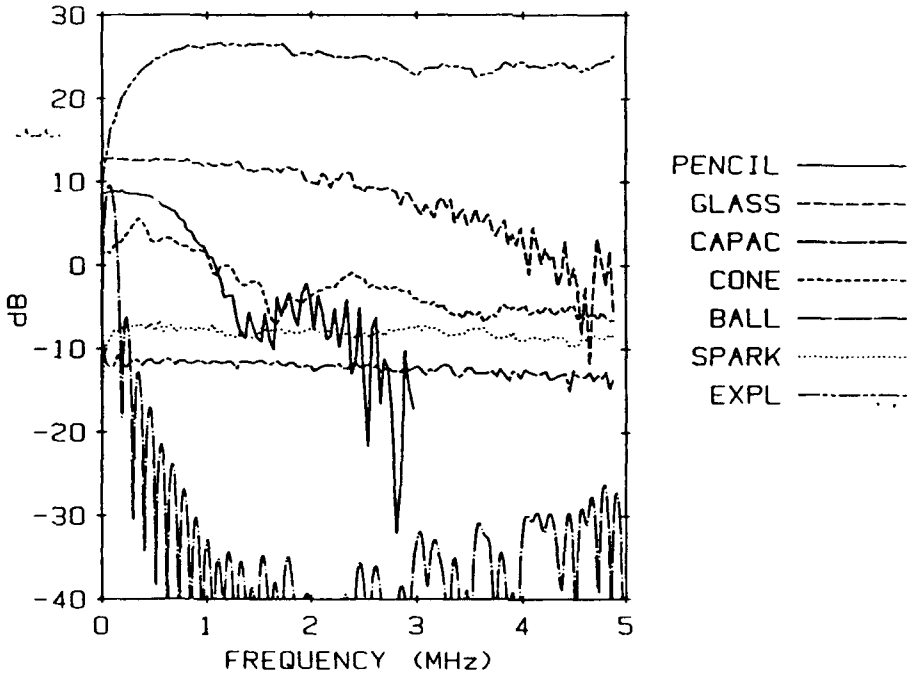

Figure 16. Typical spectra from all seven types of sources.

TABLE IV. Summary of Properties of Sources

	Risetime 0-100% (μs)	Risetime 0-90% (μs)	Damage to Plate	Variation of Force (%)	Number of Tests	Peak Force (N)
Pencil 0.2 mm	2.50	1.75	N[10]	22	4	1.01
Pencil 0.3 mm	2.50	1.35	N[10]	15	3	2.05
Pencil 0.5 mm	2.50	2.08	N[10]	5	3	2.79
Capillary 0.12 mm	0.20	0.18	Y	28	2	3.70
Capillary 0.12 mm	0.25	0.18	Y	20	5	4.03
Capillary 0.18 mm	0.35	0.27	Y	-	1	4.98
Capacitive Xdcr[1]	0.15	0.10	N	<1[13]	64	0.07
Capacitive Xdcr[2]	0.15	0.10	N	<1[13]	32	0.28
Capacitive Xdcr[3]	0.25	0.10	N	<1[13]	32	0.12
Conical Xdcr #4[4]	0.60	0.38	Y	<1[13]	32	-1.63
Conical Xdcr #5[4]	0.63	0.45	Y	<1[13]	32	-1.58
Ball 0.79 mm	2.37	-	Y[11]	4	4	-0.52
Ball 1.59 mm	4.63	-	Y	2	10	-1.84
Ball 2.38 mm	7.00	-	Y	3	5	-3.53
Ball 3.18 mm	9.50	-	Y	3	10	-5.72
Spark[5]	0.15	0.10	Y	-	6	-0.38[14]
Spark[6]	0.10	0.10	Y	-	1	-0.16
Spark[7]	0.10	0.10	Y	-	5	-0.53[15]
Explosive[8]	0.23	0.20	Y[12]	260	5	-11.96[16]
Explosive[9]	1.03	0.95	Y[12]	2300	4	-4.98[17]

1 Standard Capacitive Source Transducer, +50 V step
2 5 mm diameter backplate, 4 μm polycarbonate dielectric, +200 V step
3 10 mm diameter backplate on polycarbonate shims, air dielectric, +170 V step
4 Driven by +100 V step
5 Variable-gap series of tests
6 Critically damped discharge (R = 3.3 ohms)
7 Variable C series of tests
8 Triggered by nearby soldering iron
9 Triggered by focussed laser beam
10 No damage occurs provided the metal pencil is not allowed to impact the plate
11 Damage not visible, but inferred from results from larger balls
12 Products from the chemical reaction were corrosive to the aluminum
13 Not determinable from averaged data; estimated from recorder characteristics
14 Values ranged from -0.24 N to -0.43 N, for gaps between 0.1 mm and 0.6 mm
15 Values ranged from -0.24 N to -0.73 N, for C = 1.8 nF to 9.1 nF
16 Values ranged from -5.17 N to -18.8 N
17 Values ranged from -0.41 N to -10.0 N

Damage to the plate was assessed by inspection with a 4X loupe after each series of tests; the presence of any visible mark was denoted in Table IV by "Y". We observed dents in the surface resulting from the ball and capillary sources, discoloration from the spark sources, and pitting from the explosive sources. The conical transducer left a barely visible mark on the polished surface of the plate. In our total series of tests, the potential effects of changes in the test surface were minimized by testing the sources in ascending order of anticipated surface damage: capacitive transducer, pencil, conical transducer, ball, spark, capillary, explosive. The marks left by any of the first six seemed insufficient to affect the results of the subsequent tests.

Representative spectra for all of the seven sources are shown in Figure 16. The spectral magnitudes span a range of 70 dB, the upper limit of which is set by the clipping level of our electronic instrumentation. Greater magnitudes are possible, especially for the capillary and explosive sources, but greater damage to the plate would be the penalty. The ball source had spectral magnitudes that were very low at high frequencies and had multiple zeros. The capacitive transducer, spark, capillary, and explosive sources are notable for the flatness of their spectra.

ACKNOWLEDGEMENTS

This work was supported by the National Institute of Standards and Technology and the Office of Naval Research.

APPENDICES

A. Calculation of Force for the Standard Capacitive Source

The electrostatic tensile force exerted on one plate of a parallel plate capacitor is $CV^2/2s$, where C is the capacitance, V is the voltage, and s is the distance between the plates. The gap width of the standard capacitive source transducer was determined from a measurement of its capacitance by using the parallel plate capacitor formula, $C = \epsilon A/s$, where ϵ is the dielectric permittivity of the medium (8.8594 pF per meter), and A is the area of the plate. For this transducer, $A = 1.78\times10^{-5}$ m^2, C = 95.2 pF, and s = 1.66 μm. The voltage step was 49.7 V, and the step force exerted by the transducer was 0.0709 N.

B. Calculation of the Sensitivity of the Capacitive Receiver

The charge sensitivity of the receiver is CV_p/s, where C is the receiver capacitance, V_p is the polarizing voltage, and s is the gap width. For this transducer, $A = 7.126\times10^{-5}$ m^2, C = 191 pF, V_p = 100 V, s = 3.305 μm, and the calculated sensitivity is 5.78×10^{-3} coulombs per meter.

REFERENCES

1. N. N. Hsu, J. A. Simmons and S. C. Hardy: "An Approach to Acoustic Emission Signal Analysis—Theory and Experiment", Materials Evaluation, 35, 100-106 (Oct 1977).
2. F. R. Breckenridge, C. E. Tschiegg and M. Greenspan: "Acoustic Emission: Some Applications of Lamb's Problem", J. Acoust. Soc. Am., 57(3), 626-631 (Mar 1975).
3. D. Legros, J. Lewiner and P. Biquard: "Generation of Ultrasound by a Dielectric Transducer" J. Acoust Soc. Am., 52(1), 196-198 (July 1972).
4. T. M. Proctor, N. N. Hsu and S. E. Fick: "Ultrasonic Point Source: The NBS Conical Transducer as a Driver", Activities 1985—Office of Nondestructive Evaluation. Nat. Bur. Stand. (U.S.), NBSIR 85-3187 (1985), p76.
5. K. B. Broberg: "A Problem on Stress Waves in an Elastic Plate", Trans. Royal Inst. Tech, Stockholm, Report No 139 (1959).
6. M. Sansalone and N. J. Carino: "Impact-Echo: A Method for Flaw Detection in Concrete Using Transient Stress Waves", Nat. Bur. Stand.(U.S.), NBSIR 86-3452 (Sept 1986).
7. D. A. Hutchins, K. Lundgren, R. P. Young and N. N. Hsu: "Laser Simulation of Buried AE Sources", J. Acoust. Emission, 5(3), S29-S33 (July-Sep 1986).
8. C. B. Scruby: "Some Applications of Laser Ultrasound", Ultrasonics, 27(4), 195-209 (July 1989).

9. N. N. Hsu and S. C. Hardy: "Experiments in Acoustic Emission Waveform Analysis for Characterization of AE Sources, Sensors and Structures", Elastic Waves and Non-Destructive Testing of Materials, AMD-Vol. 29, Ed. by Y. H. Pao, ASME (1978).
10. N. N. Hsu and D. G. Eitzen: "Experimental Determination of a Point Impact Force-Time Function", submitted to Experimental Mechanics.
11. N. N. Hsu and D. G. Eitzen: "The Inverse Problem of Acoustic Emission--Explicit Determination of Acoustic Emission Source Time-Functions", Review of Progress in Quantitative Nondestructive Evaluation, Vol 1, Ed by D. O. Thompson and D. E. Chimenti (Plenum Publishing Corporation, 1982), p405-412.
12. N. N. Hsu and D. G. Eitzen: "Acoustic Emission Source Characterization through Direct Time-Domain Deconvolution", Proc. ARPA/AFML Rev. Quantitative NDE (July 1979).
13. A. S. Carasso and N. N. Hsu: "Probe Waveforms and Deconvolution in the Experimental Determination of Elastic Green's Functions", SIAM J. Appl. Math. 45(3), 369-382 (June 1985).
14. Y-H Pao, R. R. Gajewski and A. N.Ceranoglu: "Acoustic Emission and Transient Waves in an Elastic Plate", J. Acoust. Soc. Am., 65(1), 96-105 (Jan 1979).
15. N. N. Hsu: "Dynamic Green's Functions of an Infinite Plate - A Computer Program", Nat. Bur. Stand. (U. S.), NBSIR 85-3234 (Aug 1985).
16. N. N. Hsu, T. M. Proctor, D. G. Eitzen and A. S. Carasso: "Experimental Green's Function and the Inverse Problem", Nat. Bur. Stand. (U.S.), NBSIR 85-3187, 71-75 (1985).
17. C. B. Scruby and H. N. G. Wadley: "A Calibrated Capacitance Transducer for the Detection of Acoustic Emission", J. Phys. D (Appl. Phys.), 11, 1487-1494 (Feb 1978).
18. F. R. Breckenridge and M. Greenspan: "Surface-Wave Displacement: Absolute Measurements Using a Capacitive Transducer", J. Acoust. Soc. Am., 69(4) 1177-1185 (Apr 1981).
19. K. Y. Kim and W. Sachse: "Self-Aligning Capacitive Transducer for the Detection of Broadband Ultrasonic Displacement Signals", Rev. Sci. Instrum., 57(2), 264-267 (Feb 1986).
20. K. Y. Kim, L. Niu, B. Castagnede and W. Sachse: "Miniaturized Capacitive Transducer for Detection of Broadband Ultrasonic Displacement Signals", Rev. Sci. Instrum., 60(8), 2785-2788 (Aug 1989).
21. J. Waldmeyer: "Fast Fourier Transform for Step-Like Functions: The Synthesis of Three Apparently Different Methods", IEEE Trans. Instrum. Meas. IM-29(1), 36-39 (Mar 1980).
22. Friedrich and Dimmock, Inc., Millville, New Jersey 08332, USA.
23. T. M. Proctor: "An Improved Piezoelectric Acoustic Emission Transducer", J. Acoust. Soc. Am., 71(5), 1163-1168 (May 1982).
24. T. M. Proctor: "Some Details on the NBS Conical Transducer", J. Acoust. Emission, 1(3), 173-178 (July 1982).
25. H. Hertz: J. Reine Angew. Math., 92, 156 (1881) (Reprinted in an english translation as Hertz's 'Miscellaneous Papers'), Macmillan, London.
26. W. Goldsmith: "Impact", Edward Arnold, Ltd., London (1960), Chapter IV.
27. D. J. Buttle and C. B. Scruby: "Characterisation of Particle Impact by Quantitative Acoustic Emission", Harwell Lab., Oxfordshire, OX11 ORA, England, Report AERE R 13028.
28. T. M. Proctor: "Measurement of Elastic Impact of Spheres", to be submitted for publication in Experimental Mechanics.
29. W. F. Ehret: "Smith's College Chemistry", 6th Ed. (1946), D. Appleton-Century Co., New York and London, p350.